1      **Supporting Information for**

2      **High-Resolution Spatial Distribution of Redox-Active Species in Arctic Sediment**
3                                          **Porewaters**

4              Jeffrey M. Hudson[1], Alexander B. Michaud[2], D. Emerson[2], Yu-Ping Chin[1*]

5      [1] *Department of Civil & Environmental* Engineering, *University of Delaware, Newark, Delaware*
6          *19716, USA* [2] *Bigelow* Laboratory *for Ocean Sciences, East Boothbay, Maine, 04544, USA*

7                              *corresponding author: yochin@udel.edu*

8

9  **Working Electrode Fabrication:**

10         Hg/Au electrodes were tailored for use in both sediment and aquatic environments. To

11  construct the electrodes, BNC cable (Newark Electronics) was stripped down to copper

12  conductor wiring, which was then fixed and soldered to 100 µM gold wire (Alfa). The length of

13  the BNC cable that was stripped and soldered to the gold wire was based on preference, although

14  at least 10 inches total is preferable for sediment work.  PEEK™ tubing (0.125") of the same

15  length as the stripped down copper plus gold wiring was used to house soldered copper and gold

16  wiring and provide protection to the wire. Before placing the soldered wiring into the PEEK™

17  tubing, a two-part epoxy mix made of 105 resin and 205 hardener (West Marine) in a 4:1 ratio

18  was mixed and immediately injected via syringe into a sectioned piece of PEEK™ tubing.

19  PEEK™ tubing was clamped into a ring stand vertically, and special care was taken to inject the

20  epoxy mix into the bottom of the tubing upwards slowly enough to ensure that no air bubbles

21  formed in the epoxy. The soldered copper and gold wire from the BNC cable was then slowly

22  lowered into the PEEK™, with the gold wire tip was positioned to be either flush or slightly past

23  the bottom of the PEEK™ tubing. Pulling the wire through the PEEK™ tubing allowed the BNC

24  cable to become flush with the top tip of the PEEK™, ensuring a good connection. Following

25  this step, fresh electrodes filled with epoxy were allowed to harden overnight.

26        Following overnight hardening, the gold tips of the electrodes were polished by hand

27  using a progression of coarse to fine grained sandpaper (100 to 1000 grit) mounted on a Dremel

28  rotary tool, followed by 15, 6 , 1, ¼ micron diamond pastes (Buehler) on mounted polishing pads

29  (Buehler) on the Dremel tool. It is imperative that Buehler diamond pastes are used in this step,

30  as aluminum abrasives used in commercial electrodes will negatively affect the plating process.

31  Briefly, a small dab of the paste is added to the polishing pad and softened with two drops of

32  polishing oil (Buehler), turning the paste into a soft slurry. Electrodes could be firmly pressed

33  vertically by hand against the rotating Dremel tool in a "figure 8" motion or held in place with a

34  micromanipulator above and assisted by hand, in small figure 8's. Typical polishing times for

35  each sandpaper and paste lasted no longer than 90 seconds.

36        Immediately following polishing, working electrodes were plated with Hg by placing the

37  working, reference, and counter electrodes in an argon-purged solution of 0.16 M $Hg(NO_3)_2$

38  dissolved in pH 1.5 deionized water (adjusted with nitric acid) while fixing the potential at -1.0

39  V for 4 minutes. This step reduces the $Hg^{2+}$ onto the Au surface of the electrode. It is important

40  to use a fritted Ag/AgCl reference electrode in this step, as solid-state Ag/AgCl electrodes will

41  dissolve in the plating solution. Following 4 minutes of Hg plating, an amalgamation step was

42  performed by placing the working electrode and Pt-wire counter electrode in a 0.1 M NaOH

43  solution for 1 minute at a potential of -9 V for the working electrode, and +9V to the counter

44  electrode. The visible formation of bubbles was $H_2$ gas, confirming reduction of water at the

45  mercury tip, thus also confirming the amalgamation of Hg onto the Au surface (Brendel and

46  Luther 1995). Successfully plated electrode tips examined under a stereo microscope had a

47  noticeably dull silver tarnish, whereas un-plated gold wire tips were gold and shiny in color.

48  Finally, after the amalgamation step, the plated working electrode, along with the platinum

49 counter and an Ag/AgCl reference electrode were placed in a 0.02 M NaCl solution and tested in

50 cyclic voltammetry mode from -0.1 to -1.8 to -0.1 V 50 to 100 times at 1 V/s in order to check

51 for the existence reproducible $O_2$ peaks (Figure S3A).

**Electrode Calibration**

53      Electrode calibrations for $O_2$, Fe(II), and Mn(II) were performed using Toolik Lake water

54 from the three sites in order to accurately represent locations where the electrodes would be used

55 in the field. $O_2$ calibrations were performed based on previously detailed methods (Moore et al.

56 2009, Hudson et al. 2019). Briefly, lake water was purged to 100% $O_2$ saturation for 1 to 2 min

57 with a small aquarium bubbler. Upon saturation, CV scans were performed and $O_2$ peak heights

58 were measured was recorded. Concentrations of $O_2$ were calculated and corrected for salinity and

59 temperature based on the equation from Weiss (1970)

$$ln[C] = A1 + A2 * \left[\frac{100}{T}\right] + A3 * ln\left[\frac{T}{100}\right] + A4\left[\frac{T}{100}\right] + S‰\left[B1 + B2\left(\frac{T}{100}\right) + B3\left(\frac{T}{100}\right)^2\right]$$

60
61          (1)

62 Because the ionic strength of Toolik Lake water was low (specific conductivity = 70 μS),

63 unaltered waters were nearly at $O_2$ saturation (DO unaltered water ~314 μM = 90% saturation:

64 100% saturation = 352 μM). A two-point calibration curve was then built from 100% $O_2$

65 saturation peak height (nA) vs ) 0 nA for a 0% saturation concentration and used to calculate

66 dissolved $O_2$ throughout the core. Porewater ionic strength were similar to Toolik Lake surface

67 water and temperatures were uniform throughout cores (data not shown).

68      Aqueous Fe(II) and Mn(II) calibrations were performed by spiking in aliquots of a 10

69 mM stock solution into a 50 ml Falcon tube filled with unfiltered Toolik Lake water. Water was

70 purged with argon before and during calibrations to prevent oxidation of Fe(II) and Mn(II).

71  Additionally, a small amount of dithionite was added to the Fe(II) stock in order to prevent

72  oxidation. While this step produced a visible FeS peak around -1.1 V, it did not interfere with the

73  Fe(II) peak around -1.43 V.  Soluble Fe(III)-organo-complexes were not quantified and reported

74  only as measured current (nA) due to the lack of a proper standard since the nature of these

75  complexes are not known.

76  **Electrode Measurement Validation**

77          To corroborate our voltammetric measurements we measured dissolved Fe(II) and

78  Fe(III) *ex situ* by the Ferrozine colorimetric analysis. Samples taken from our Rhizon sampler

79  integrated the top 5 cm of the gully water column where we observed lower concentrations for

80  Fe(II) (27.2 µM) while Fe(III) was 14.1 µM.  Our Rhizon results corroborate the existence of

81  both Fe(II) *and* Fe(III) as detected by the microelectrode, but the Rhizon measurements are less

82  due to some oxidation artifacts despite our attempts to preserve the sample quickly with HCl.

83  Because of the near circumneutral iron seep pH even small amounts of $O_2$ diffusion could

84  oxidize some of the Fe(II). Further, because the Rhizon approach is a composite sample it

85  represents an average of Fe(II) concentrations unlike our microelectrode that measures the

86  analyte at its tip. Thus, while the *in situ* measurement of redox sensitive species using

87  voltammetric microelectrodes provides finer spatial resolution, one must make many more

88  measurements over a larger space to capture Fe(II) concentrations in the solution volume

89  determined by the Rhizon sampler. Nonetheless, the Fe(II) value measured using the Rhizon

90  collected porefluids still compares favorably (within 64%) to the voltammetrically obtained

91  value.

92

93

**Solid Phase Fe(III) Abundance Calculation**

We determined the amount of solid phase Fe(III) in quasi-equilibrium with porewater Fe(II)

based upon an assumed porosity ($\phi$) of 0.7 at a depth of 1cm below the SWI. Thus, at this depth

the Fe(III) solid phase concentration is 60 µMol/g from Figure 3 and the porewater Fe(II)

concentration is 10 µM. Based upon our assumed porosity the sediment-to-water concentration

(SW) is

$$SW\ (kg/L) = \rho_s[(1 - \phi)/\phi]$$

Where $\rho_s$ = the density of a sediment solid ($\sim$ 2.5kg/L) (Schwarzenbach et al., 2017). Our SW

value would be 1.07kg/L or 1.07 g/mL or 1 gram of sediment will have 0.93 mL of porewater

associated with it. The total **moles** of Fe(II) at 1cm would be $9.3 \times 10^{-3}$ µMoles, while the solid

phase concentration would contain 60 µMoles. Thus, there is abundant Fe(III) available to the

iron reducers present in this sediment layer. Even much deeper in the core there exist sufficient

Fe(III) to support iron reduction. Using the same logic, but a different porosity (0.5) at a depth

of 5 cm the solid phase Fe(III) concentration is $\sim$ 7 µMol/g, while the porewater concentration is

$\sim$ 300 µM. The SW value would be 2.5 g/mL. Thus, the total moles of Fe(III) would be $\sim$ 17.5

µMoles (based upon a mass of 5.8g), while the moles of Fe(II) in 1 mL of porewater would be

0.3 µMoles. Thus, even at depth sufficient solid phase enough Fe(III) exists to support iron

reducers until it is below the detection limit of our analytical method.

112

113     Figure S1. Field laboratory set-up of ex-situ voltammetric sediment core analysis.
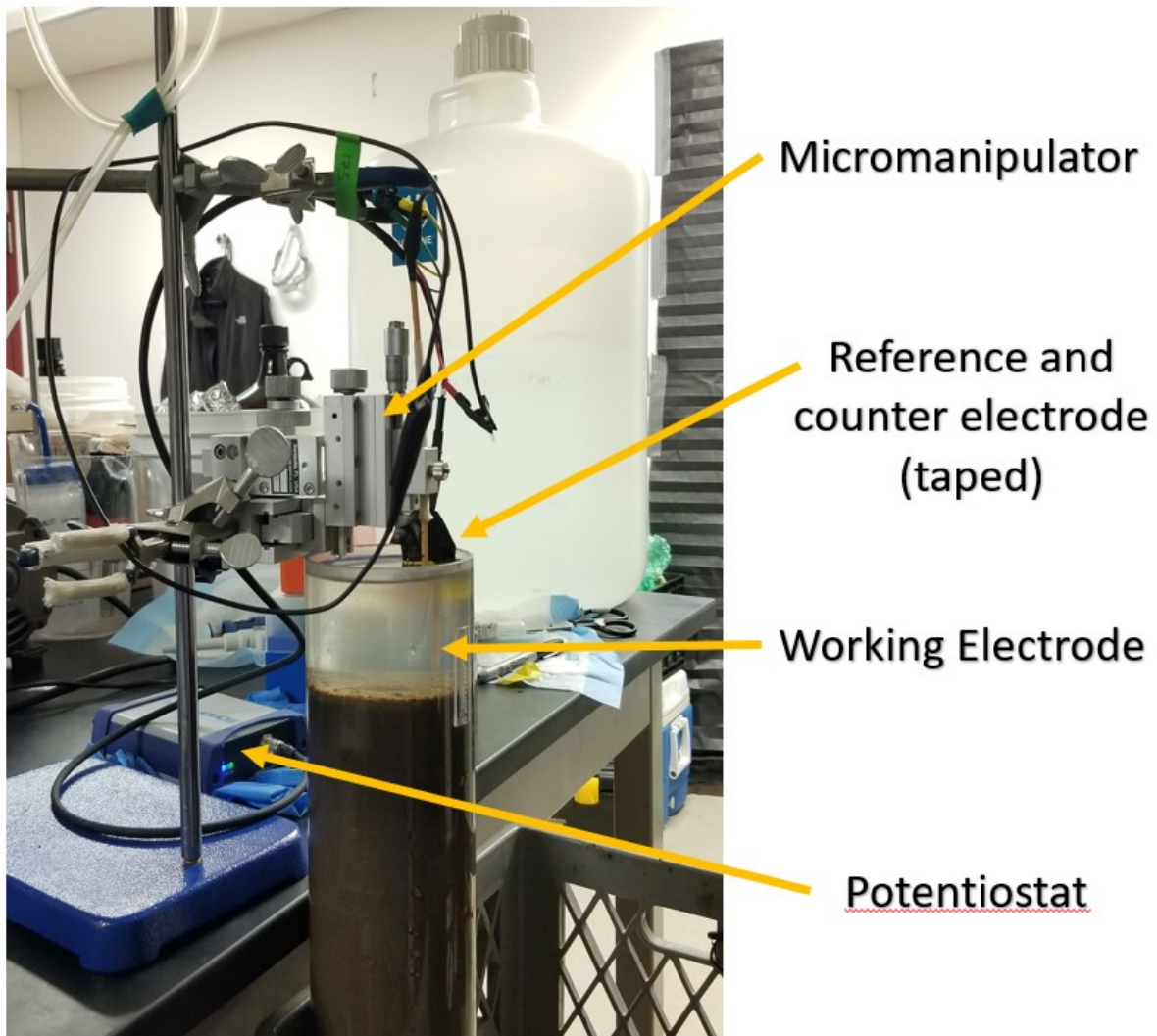


114

115

116

117

118

119

120

121

122

123

124    Figure S2. Iron seep at Oksrukuyik River.
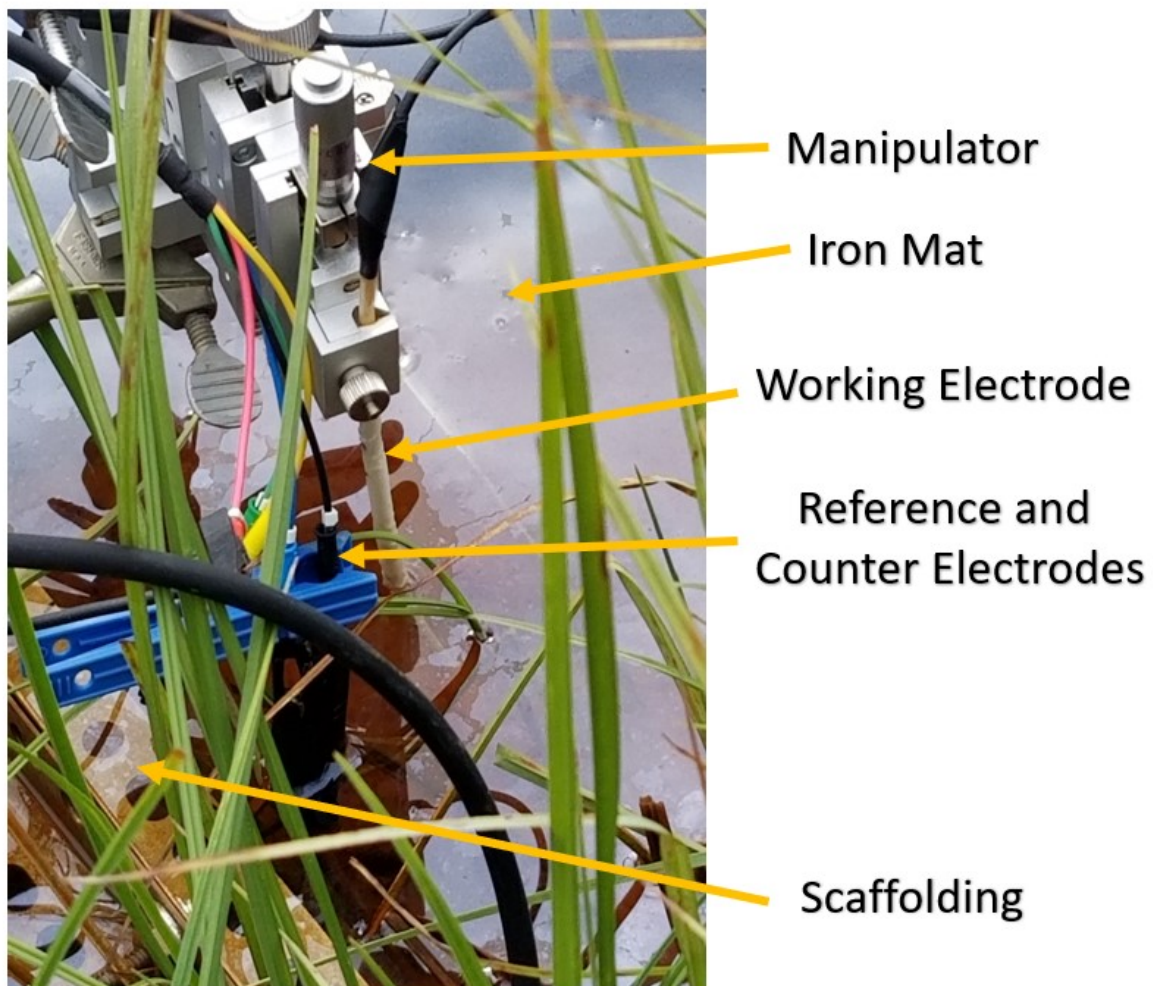


125

126

127

128

129

130   Figure S3. Oks iron seep field experimental setup.



131

132

133

134

135

136

137

138

139 Figure S4. Representative cyclic voltammograms of species present directly in Toolik Lake and

140 Arctic freshwater samples. A) $O_2$ (half-wave potential ~ -0.33 V) signal response from Toolik

141 Lake surface water B) $Fe^{2+}$ (half-wave potential -1.43 V) measured from a Toolik sediment core

142 C) $Fe^{2+}$ and $Fe^{3+}$ (present as DOM complex anywhere from -0.4 to -0.9V; -0.5 V here) measured

143 in an iron seep near Oks D) Toolik Lake sediment core scan showing peaks for Mn(II) (half-

144 wave potential at -1.55 V), small concentration of Fe(II) (-1.43), and an Fe(III)-complex (-0.65
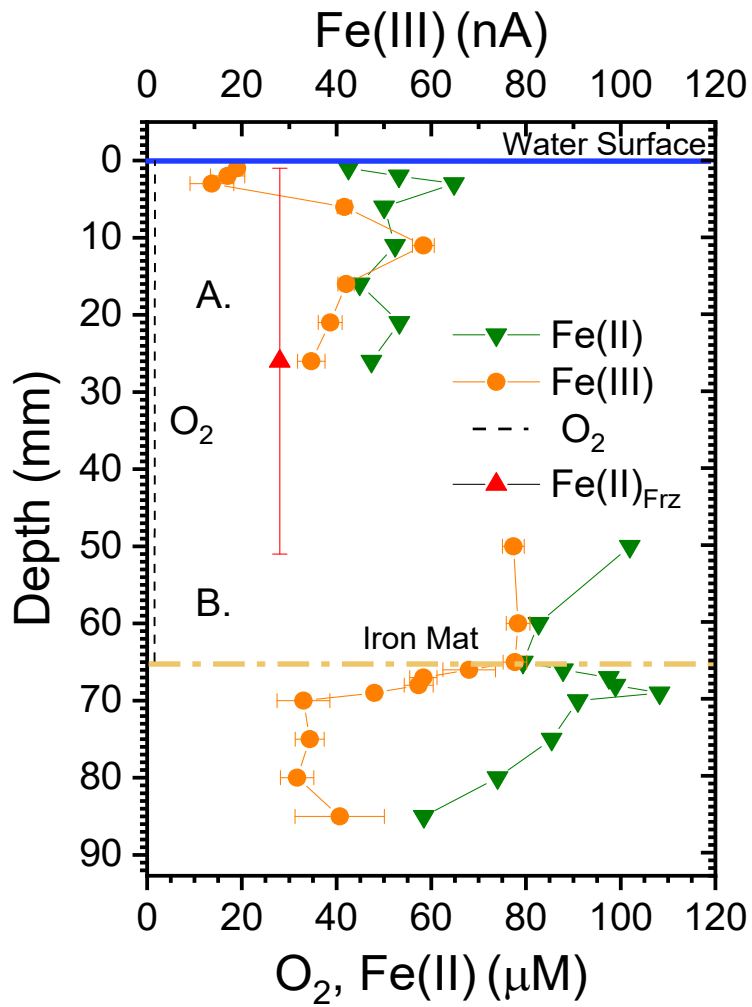
145 V).
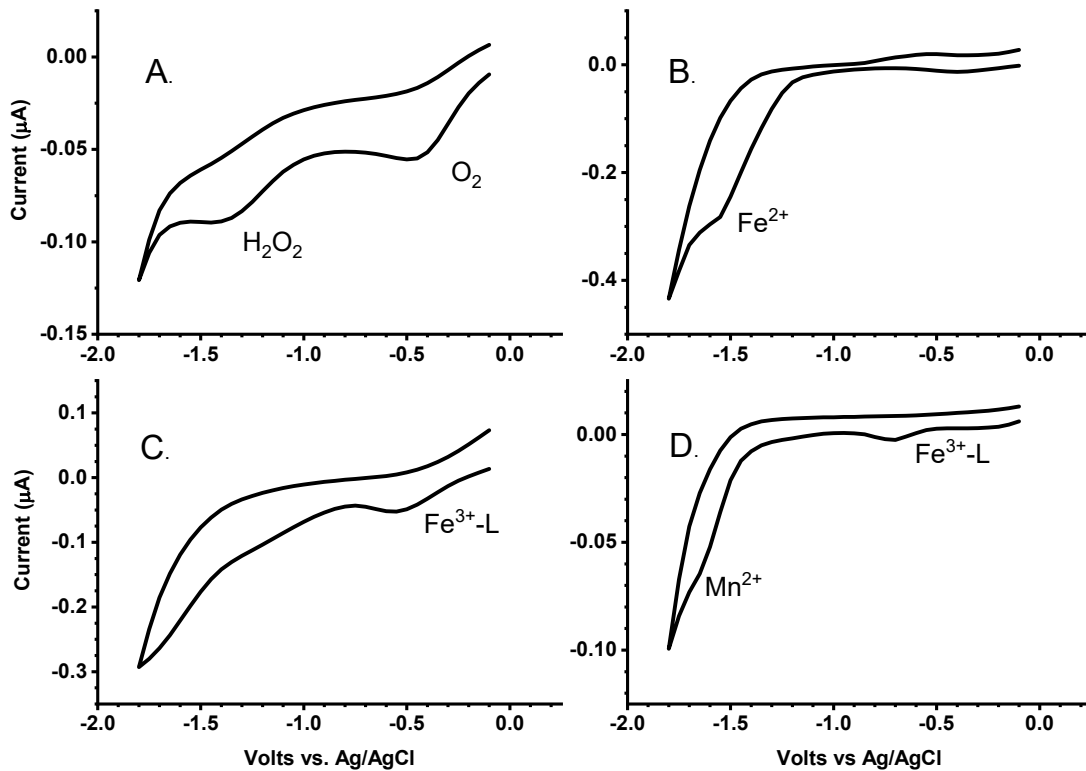


146
147

148

149

150 Figure S5. Validation of electrode measurements with Ferrozine assay. An Fe(II) measurement made by

151 Ferrozine assay (Fe(II)$_{Fero}$) is shown by the red triangle. Vertical error bars on the Ferrozine measurement

152 represent the 5 cm integration of vertical space created by the measurement

153



154
155

156

157

158

159   Figure S6. Cores taken around Toolik Lake. Measurements for $O_2$, Fe(II), and Mn(II) are in μM,

160   while Fe(III) measurements are reported by current (nA). Note y-axis scales are not uniform in

161   depth, and x-axis scales are not uniform in concentration. Cores are divided by shallow, near

162   shore cores (top row), and deeper, middle lake cores (bottom row).

163
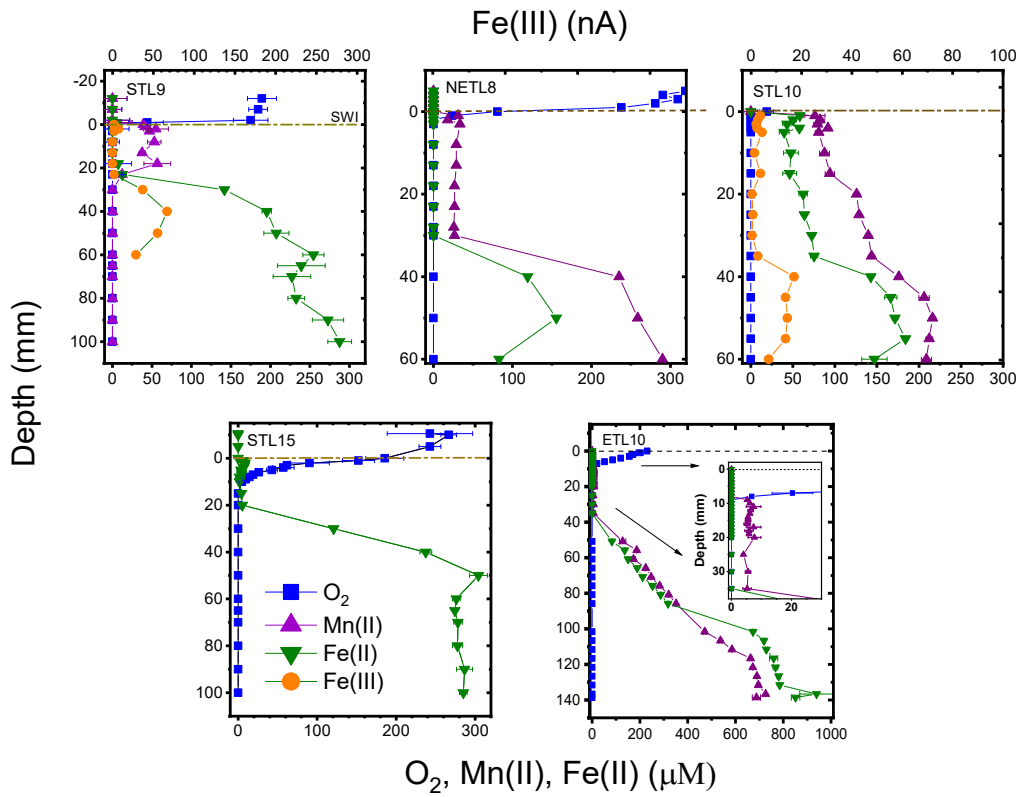


164

165    Figure S7. Iron oxides at the sediment-water interface from Core 2.
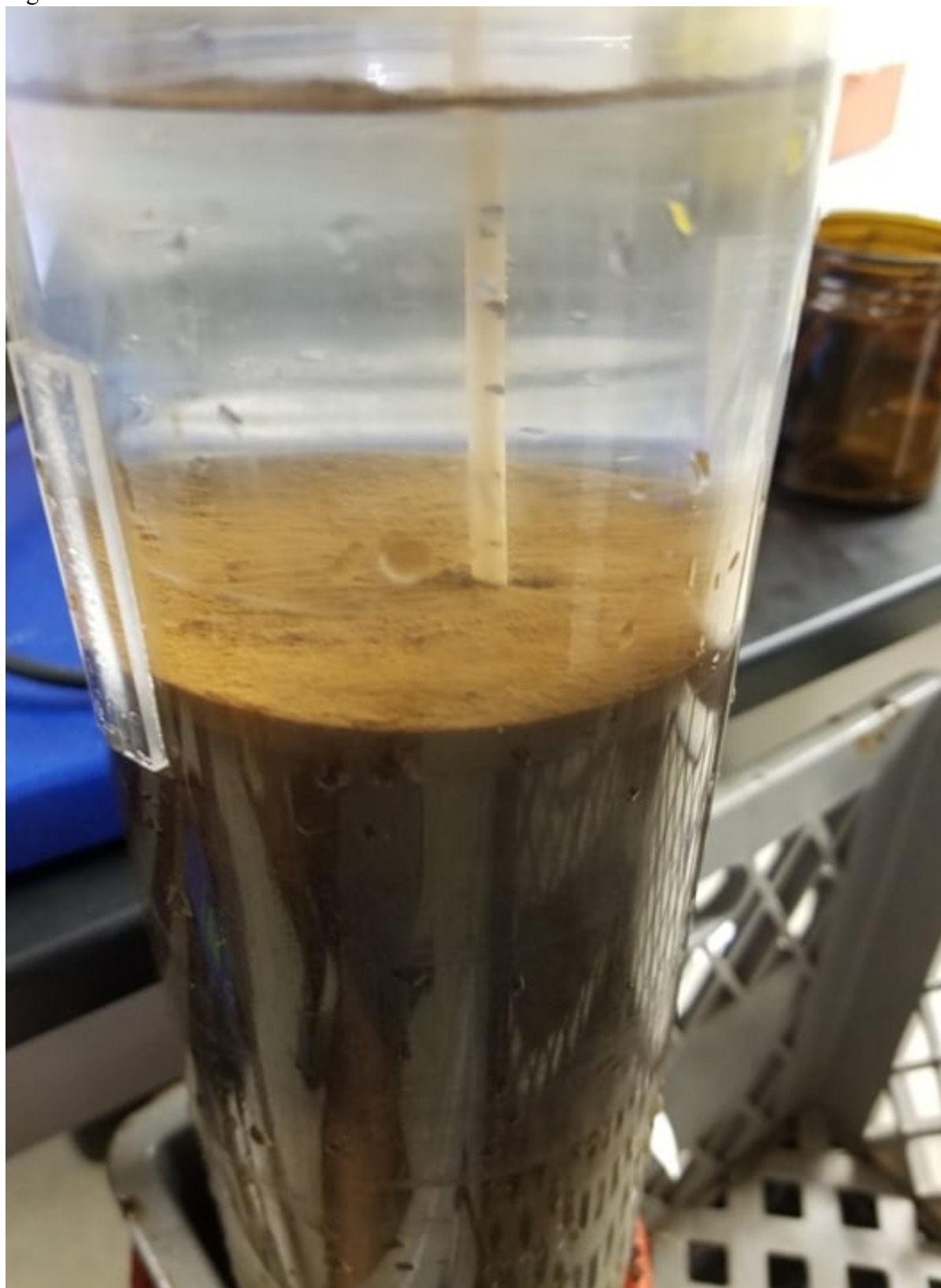


166

167 **References**

168    1)  P.J. Brendel and G.W. Luther, Development of a gold amalgam voltammetric

169         microelectrode for the determination of dissolved Fe, Mn, O2, and S (-II) in porewaters

170         of marine and freshwater sediments, *Environ. Sci. Technol.*, 1995, **29**, 751-761.

171    2)  J.M. Hudson, D.J. MacDonald, E.R. Estes, and G.W. Luther, A durable and inexpensive

172         pump profiler to monitor stratified water columns with high vertical resolution, *Talanta*,

173         2019, **199**, 415-424.

174    *3)*  T.S. Moore, D.B. Nuzzio, D.M. Di Toto and G.W. Luther, Oxygen dynamics in a well-

175         mixed estuary, the lower Delaware Bay, USA, *Mar. Chem*, 2009, **117**, 11-20.

176    4)  R.P. Schwarzenbach, P.M. Gschwend and D.M. Imboden, in *Environmental Organic*

177         *Chemistry*, ed. J. Wiley and Sons, 3rd edn., 2016.

178    5)  R.F Weiss, The solubility of nitrogen, oxygen and argon in water and seawater, *Deep Sea*

179         *Research and Oceanographic Abstracts*, 1970, **17**, 721-735.

180

181

182
183